

Effects of O₂ addition on in-plasma photo-assisted etching of Si with chlorine F

Cite as: J. Vac. Sci. Technol. A 38, 053003 (2020); doi: 10.1116/6.0000338

Submitted: 14 May 2020 · Accepted: 10 July 2020 ·

Published Online: 30 July 2020



View Online



Export Citation



CrossMark

Linfeng Du, Emilia W. Hirsch, Demetre J. Economou,^{a)} and Vincent M. Donnelly^{b)}

AFFILIATIONS

Plasma Processing Laboratory, Department of Chemical and Biomolecular Engineering, University of Houston, Houston, Texas 77204

Note: This paper is part of the Special Topic Collection Commemorating the Career of John Coburn.

^{a)}Electronic mail: economou@uh.edu

^{b)}Electronic mail: vmdonnelly@uh.edu

ABSTRACT

Addition of oxygen was used to control the in-plasma photo-assisted etching (PAE) of *p*-type Si(100) and poly-Si in a high density, inductively coupled, Faraday-shielded, Ar/Cl₂ (225/25 SCCM), 60 mTorr plasma. After etching, samples were transferred under vacuum to an UHV x-ray photoelectron spectroscopy chamber for surface analysis. Samples etched under PAE conditions (ion energies below the ion-assisted etching, IAE, threshold) had a thicker surface oxide and lower [Cl] surface concentration, when compared to samples etched under IAE conditions (ion energies above the IAE threshold). PAE was found not to be affected by 0.1 or 0.25 SCCM O₂ addition, while etching stopped with more than 0.5 SCCM O₂ addition. IAE with RF power on the sample stage, resulting in -65 V self-bias, was not affected by up to 2 SCCM of oxygen addition but decreased rapidly when more than 5 SCCM O₂ was added to the plasma. These results imply that PAE may be completely suppressed, while IAE occurs unobstructed. The implications of these findings are discussed in view of applications involving continuous wave and pulsed-plasma processes.

Published under license by AVS. <https://doi.org/10.1116/6.0000338>

I. INTRODUCTION

Reactive ion etching (RIE) is widely used to delineate fine features in the manufacturing of integrated circuits.^{1–3} Coburn and Winters first reported in 1979 the synergistic effect of simultaneous exposure of an Si surface to energetic ions and neutral etchants.⁴ At high ion energies (e.g., 100 s of eV), ions play a dominant role in etching, while electrons and photons are of secondary importance.^{5–8}

Operating at low (10 s of eV) ion bombardment energies, however, is critical to improve selectivity and minimize substrate damage during RIE, especially in the manufacturing of nanoscale devices. For example, it has been reported that the selectivity of Si with respect to SiO₂ could reach 100:1 near the threshold for ion-assisted etching.^{3,9} At such low ion energies, ion-assisted etching may not be the dominant contributor to etching. In previous work, Shin *et al.* first reported the important contribution of in-plasma photo-assisted etching (PAE) of *p*-type Si in chlorine-containing plasmas.¹⁰ It was found that in Ar plasmas mixed with a few

percent of Cl₂, etching persisted below the ion-assisted etching threshold (16 eV). The subthreshold etching rate was independent of ion energy and was attributed mainly to plasma-generated vacuum ultraviolet (VUV) photons. Zhu *et al.* demonstrated that photo-assisted etching of *p*-type silicon occurred in plasmas containing Cl₂, Br₂, HBr, Br₂/Cl₂, and mixtures with Ar.¹¹ In all these cases, a significant etching rate below the threshold ion energy was observed. Sridhar *et al.* used power modulation to obtain further insight into the PAE mechanism.¹² Etching under pulsed DC bias provided evidence of antisynergism between PAE and ion-assisted etching (IAE), which was attributed to energetic ions creating damage on the surface, which enhanced recombination of electron-hole pairs, thereby reducing the photo-assisted etching rate.¹³

Depending on the process, PAE can be advantageous or detrimental. For example, PAE was used for highly selective, high aspect ratio etching of nanofeatures into Si, with the native oxide as the masking layer.¹⁴ On the other hand, PAE can have a negative impact on self-limiting processes such as atomic layer etching

(ALE). PAE could compromise the self-limiting nature of the first step of ALE, namely, reactant chemisorption.^{15,16}

Oxygen addition to plasmas has been studied for decades, due to its ability to increase etchant concentrations (e.g., F-atom density in a CF₄ plasma¹⁷), improve anisotropy and control feature profiles shapes by forming sidewall protection layers, and improve selectivity by suppressing surface reactions.^{17–22} The suppression of Si etching in halogen-containing plasmas by the addition of O₂ has been widely reported. Zau and Sawin investigated the effects of O₂ addition in Cl₂ plasma etching of polysilicon.²⁰ They found that the etching rate under energetic ion bombardment can be either enhanced or reduced by the addition of O₂. The initial enhancement (up to 2% added oxygen) was attributed to reactor wall conditioning by deposition of an oxychloride film that reduced surface recombination of Cl atoms, enhancing their concentration in the reactor. Too much O₂ addition (6–10%), however, led to the formation of a relatively thick surface oxide layer. Cl₂ plasmas are very selective in etching Si over SiO₂, hence the oxide layer stopped etching. Cheng *et al.* found that the silicon etching rate decreased rapidly above 20% added O₂ in a Cl₂/O₂ inductively coupled plasma (ICP) (substrate bias voltage was –34 V), due to excessive oxidation of the surface and formation of a nonvolatile silicon oxychloride SiCl_xO_y layer.²³ Tuda and Ono reported that 25% O₂ in a Cl₂/O₂ plasma with a ~100 V RF bias stopped poly-Si etching, which was also attributed to the formation of the oxide layer.²⁴ Kuroda and Iwakuro showed that the ion-assisted etching rate of poly-Si in HBr/O₂ plasmas was enhanced with increasing O₂ addition up to 25%, but then abruptly decreased by a factor of 16 above 30% O₂, as the oxide layer becomes too thick for fast etching to occur.²² They attributed the increasing etching rate up to 25% O₂ addition to an increase in Br⁺ concentration. Donnelly *et al.* used vacuum transfer x-ray photoelectron spectroscopy (XPS) to study oxidation of Si under thin SiO₂ films in an HBr/O₂ plasma.¹⁹ They found that the oxide film would either grow or etch, depending on the initial layer thickness. A ~30 Å thick oxide, resulted in the etching rate balancing the growth rate.

In the present work, the effects of adding small amounts of oxygen on the etching rate of silicon in an Ar/Cl₂ plasma were explored under conditions that lead to etching driven either by energetic ion bombardment or due to in-plasma photo-assisted surface reactions. XPS, with sample transfer under vacuum, was used to determine the degree of surface chlorination and oxide layer thickness.

II. EXPERIMENTAL APPARATUS AND PROCEDURES

The experimental apparatus used in this study is shown schematically in Fig. 1. An ICP was generated in an alumina tube (33 cm long, 7.94 cm inside diameter) powered by a 4-turn air-cooled copper coil. 13.56 MHz continuous wave power generated by a function generator (Keysight, 33600A) and an RF amplifier (ENI A500), was supplied to the reactor through a Π-matching network. The net (forward minus reflected), nominal ICP power was 350 W. A Faraday-shield prevented capacitive coupling between the high voltage coil and the plasma, suppressing plasma potential oscillations, thereby simplifying control of the energy of ions bombarding the sample. The water-cooled sample stage could

be grounded or powered by RF or DC. When 14.5 MHz RF power, generated by a function generator (Stanford Research Systems, DS345) and an RF amplifier (ENI, A150), was applied to the sample stage, through a Π-matching network, a negative self-bias voltage was generated.

The plasma reactor was pumped by a 300 l/s turbomolecular pump (Ebara, ET300W), and the base pressure was 4×10^{-7} Torr. Gases were injected into the plasma chamber from a nozzle in the top flange. The chlorine (Matheson, 99.99% purity, 25 SCCM) and argon (Matheson, 99.999% purity, 225 SCCM) flow rates were regulated by using mass flow controllers (Mykrolis, FC-2979). Oxygen (Matheson, 99.98% purity) flow was regulated by a mass flow controller (STEC, SCE-7330) for flows at or above 1 SCCM or by a needle valve (Vacuum Generators, MD7) for flows less than 1 SCCM. Gas pressure was maintained at 60 mTorr, as measured with a capacitance manometer (MKS 629, 0.1 Torr full scale), by throttling the gate valve of the plasma chamber.

Silicon samples (~1.1 × 1.1 cm²) were cleaved from a highly doped *p*-type Si (100) wafer (resistivity 0.001–0.005 Ω cm); cleaned with acetone, methanol, and DI water; and blown dry with ultrahigh purity nitrogen. Samples were then soldered to a 1.95 cm-diameter highly doped *p*-type Si cover disk (resistivity 0.001–0.005 Ω cm) over a 2.54 cm-diameter stainless steel (SS) sample holder by using a 5 × 5 × 0.05 mm-thick indium foil (Stanford Advanced Materials, 99.995% purity). The stack was annealed under a nitrogen atmosphere at 200 °C for 5 min. The sample stage cover disk was used to prevent possible contamination caused by SS sputtering. Since the sample was soldered to a water-cooled stage, ensuring good thermal (and electrical) contact, heating of the sample during etching is expected to be insignificant.

Masked samples were used for etching rate measurements via laser interferometry. The mask pattern consisted of 1 μm-thick SiO₂ lines on a *p*-type Si (100) substrate with a resistivity of 5–100 Ω cm. The pitch width (line + space) of the pattern was 100 μm at 50% density. Unpatterned poly-Si samples (1 μm poly-Si on 0.1 μm SiO₂ on a *p*-type Si substrate with a resistivity 1–30 Ω cm) were also used for etching rate measurements. After etching, unmasked Si (100) samples were transferred under vacuum from the plasma chamber to the XPS chamber (base pressure ~7 × 10^{–10} Torr) for surface analysis. Unless otherwise stated, all PAE and IAE samples analyzed by XPS were etched for 30 and 10 s, respectively.

The XPS instrument (Surface Science Instruments) used an Al x-ray source to provide a monochromatic beam ($\lambda = 0.83$ nm, which corresponds to a photon energy of 1486.6 eV) focused on the sample using a quartz crystal. In this study, spectra were obtained for takeoff angles of 30° and 85° (with respect to the plane of the sample surface), corresponding to probing depths in Si of about 8 and 22 Å, respectively.²⁵ Photoelectrons ejected from the sample were detected by an energy analyzer. XPS low resolution survey spectra were used to determine the surface elemental composition by identifying the position of the corresponding binding energy peaks, spanning the range 0–1000 eV with a 800 μm-diameter beam spot. High resolution (HR) spectra of Si (2p) were recorded in the region 96–108 eV with a 300 μm-diameter beam spot. The 85° takeoff angle HR spectra were used to estimate the silicon dioxide layer thickness by comparing

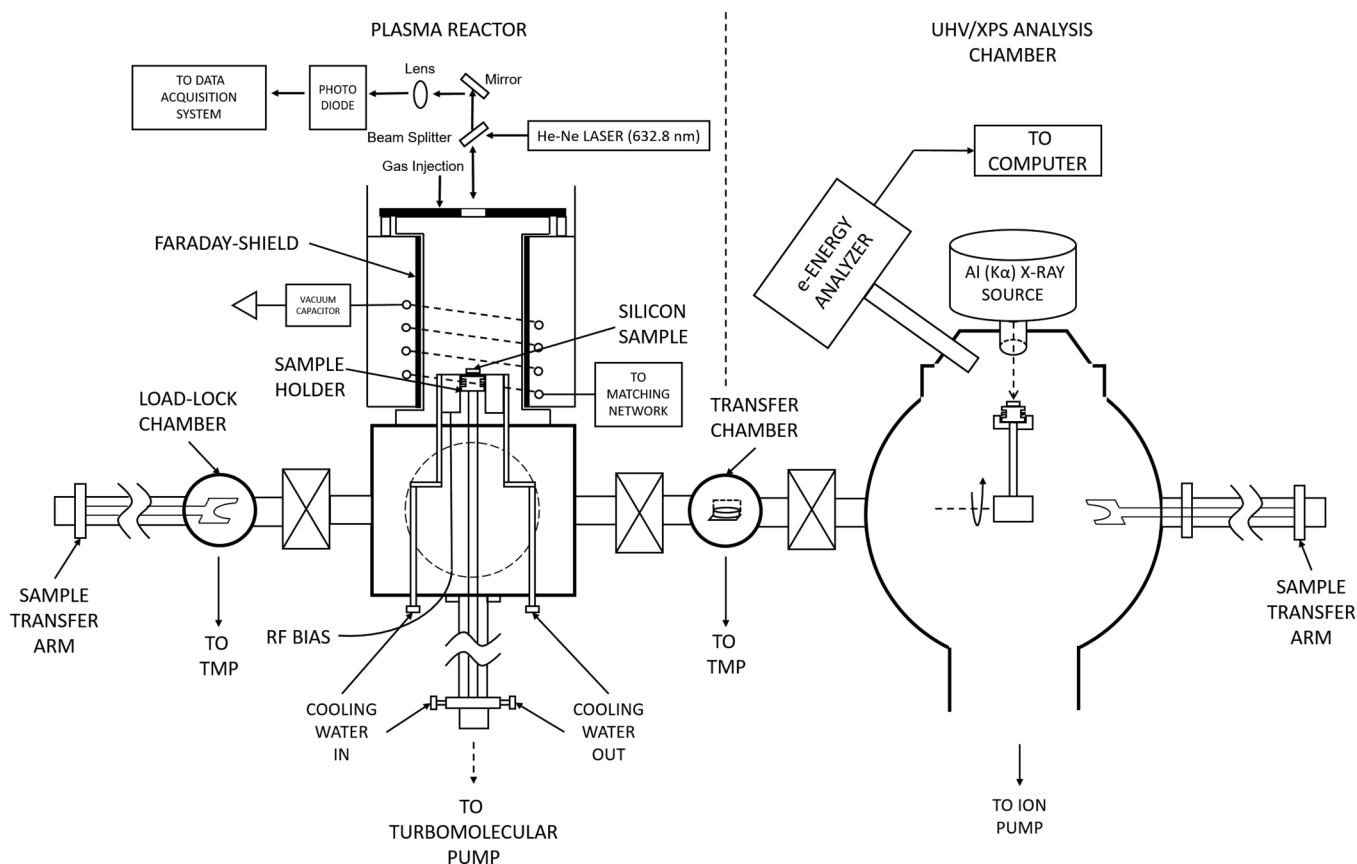


FIG. 1. Schematic of the inductively coupled plasma reactor, laser interferometry, and UHV/XPS chamber. A sample was mounted on the sample holder that could be transferred from the reactor to the XPS chamber under vacuum (TMP = turbomolecular pump).

the intensity of two major peaks in the Si(2p) region: SiO₂ (~104.5 eV) and substrate Si (99.5 eV).

Laser interferometry was used to measure the silicon etching rate *in situ*.^{26,27} The light path difference between the SiO₂ mask and the exposed *p*-type Si in a patterned sample caused modulation of the intensity of the reflected laser beam. A nonpolarized 632.8 nm He-Ne laser was directed to and reflected off the sample at normal incidence. One period of the recorded interferogram defined the depth, Δd , of etched Si, given by

$$\Delta d = \frac{\lambda/2}{\sqrt{n^2 - \sin^2 \theta}}, \quad (1)$$

where λ , n , and θ are the laser wavelength, film index of refraction, and angle of incidence with respect to the surface normal, respectively (here $\theta = 0^\circ$). For the patterned crystalline Si sample, $n = 1$ (vacuum). The same relationship holds for poly-Si thin film samples, with $n = 3.88$. Dividing Δd (etched depth) by Δt (the time interval between two consecutive peaks) gives the average etching rate over that time interval.

Provided the amount of oxygen addition was insufficient to allow a continuous oxide layer to form, the etching rate was found to be independent of time. Conversely, for intermediate oxygen additions, and depending on whether bias is on or off, the etching rate slows and then stops. For this unsteady-state situation, the first cycle of interference was used to define an initial etching rate.

III. RESULTS AND DISCUSSION

A. Effect of oxygen addition on the etching rate of silicon

Figure 2 shows an interferogram recorded during continuous exposure of a patterned *p*-type Si sample to an Ar/Cl₂/O₂ (225/25/2 SCCM) plasma. Between 0 and 25 s, no RF bias was applied to the substrate stage and no etching occurred, as indicated by the constant intensity of the reflected laser beam. From 25 to 41 s, RF bias (-45 V self-bias) was applied to the sample stage, resulting in etching of silicon at a rate of 2900 nm/min. This is comparable to the etching rate (2500 nm/min) without the addition of oxygen, suggesting that 2 SCCM of oxygen addition does not affect the etching rate obtained in the baseline Ar/Cl₂ (225/25 SCCM) plasma.

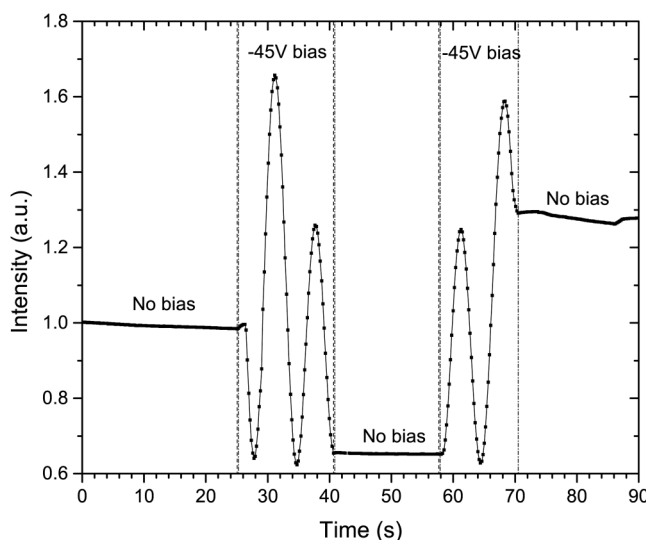


FIG. 2. Interferogram of p-type Si etching in an Ar/Cl₂/O₂ (225/25/2 SCCM) plasma. Etching occurs when the sample stage is RF-biased (-45 V self-bias), but etching stops when the RF bias is turned off.

at this bias voltage. At 41 s, bias was again turned off and the etching rate quickly dropped to zero and remained so until the same RF bias was reapplied at about 58 s, whereupon the etching rate returned to 2900 nm/min. After the RF bias was again extinguished at 71 s, little or no etching occurred. (The unequal maxima in reflected laser intensity during the two periods of etching are due to secondary interference produced by the slow etching of the SiO₂ mask.) There is a slight intensity decrease with no bias, over the time window of 70–90 s. If this is due to etching and not some other cause of drift in signal, then based on the initial and final laser intensity values over a period, the estimated Si thickness change is 16 Å, corresponding to a very small etching rate of 0.8 Å/s.

With the bias turned off (grounded sample stage), ion energies (~ 5 eV, equal to the plasma potential) were well below the IAE threshold energy of ~ 16 eV^{10,28} for etching Si in Cl₂-containing plasmas. Nonetheless, in oxygen-free Ar/Cl₂ (225/25 SCCM) plasmas, we previously found that even with no substrate bias, substantial etching occurred (typically 400 nm/min), ascribed to a VUV photo-assisted process, under these high density plasma conditions.¹³ Apparently, the addition of a small amount of O₂ leads to the formation of a thin SiCl_xO_y layer that stops photo-assisted etching. Neither 5 eV ions nor VUV photons are effective in removing this inhibiting layer. With bias applied, energetic ion bombardment apparently suppresses the formation of the SiCl_xO_y layer, allowing etching to occur at about the same rate as without O₂ addition.

Silicon etching rates as a function of oxygen addition, under a constant -65 V self-bias on the RF powered sample stage, are shown in Fig. 3. The impinging ion bombardment energy (70 V) is simply the difference between the plasma potential (~ 5 V) and self-bias voltage. In general, the etching rate decreases with increasing O₂ addition. With little or no O₂ addition (≤ 1 SCCM) etching rates were constant as a function of time.

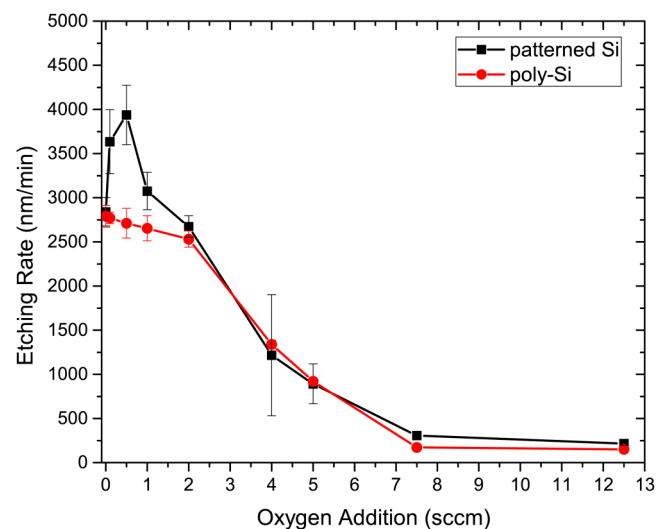


FIG. 3. Si etching rate as a function of oxygen addition with RF power on the sample stage yielding a self-bias of -65 V (ion energy of 70 eV). Ar and Cl₂ flow rates were 225 SCCM and 25 SCCM, respectively.

Though a minor point, the etching rate of patterned silicon in Fig. 3 increases somewhat with O₂ addition before falling in a manner similar to that for poly-Si. This may be due to differing reactor wall conditions caused by the deposition of an SiCl_xO_y layer in earlier experiments that reduced the heterogeneous recombination probability of Cl atoms,²⁰ thereby increasing the Cl-to-Cl₂ number density ratio, as well as the electron density through suppression of electron loss from dissociative attachment with Cl₂, both of which could increase the etching rate. These effects made it difficult to obtain precise etching rates since any given experiment depended on the prior experiments. There could also be subtle differences between the behavior of single crystal (the patterned samples) and polycrystalline Si in this region of small O₂ additions, where a transition is occurring between the oxidation rate just exceeding the oxide etching rate (an oxide layer slowly thickens) and the etching rate just exceeding the oxidation rate (resulting in no oxide growth).

The main finding is clear; however, the addition of O₂ to the plasma slows and stops etching, as reported by many researchers. Since it takes very little O₂ to suppress PAE (see Figs. 2 and 4, where it is shown that 0.5 SCCM suffices to stop PAE), while several times as much O₂ can be added before IAE is stopped, there appears to be a “window” of 1–3 SCCM of O₂ addition, where PAE is suppressed and IAE proceeds at a fast rate.

Figure 4 shows the etching rate as a function of ion energy. Monoenergetic ions were obtained by applying the pulsed negative DC bias voltage (90% duty cycle and 10 kHz frequency) on the conductive sample stage. Since the formation of a thick enough oxide layer would cause positive charging and therefore reduce the energy of ions impacting the surface, the O₂ flow rate was kept at or below 0.5 SCCM. Drifting chamber conditions again increased the scatter in the measurements. Nonetheless, it is apparent that

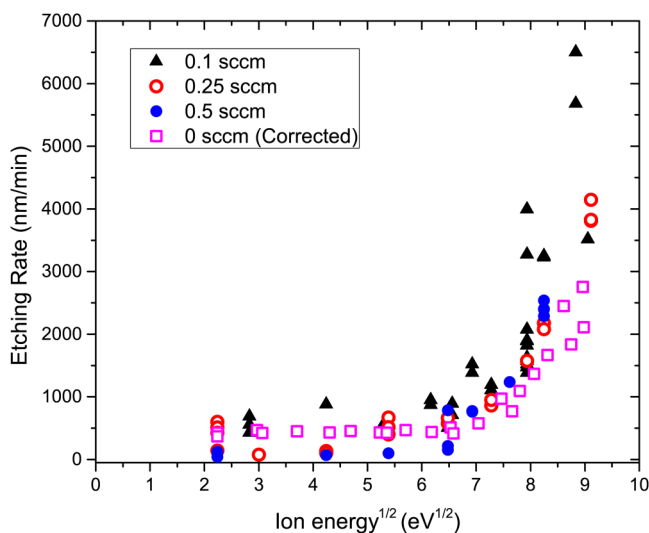


FIG. 4. Etching rate of p-type silicon as a function of the square root of ion energy with pulsed negative DC bias (10 kHz frequency, 90% duty cycle) on the sample holder. 0.1, 0.25, or 0.5 SCCM O₂ was injected into Ar/Cl₂ (225/25 SCCM) plasmas. Data for 0 SCCM O₂ addition (50% DC bias duty cycle) were obtained by previous experiments (Ref. 13) with the IAE rates multiplied by 9/5 to correct for the duty cycle difference.

PAE always occurred for oxygen additions of 0 and 0.1 SCCM, sometimes occurred with 0.25 SCCM O₂ addition, but was always nearly extinguished with oxygen additions of 0.5 SCCM, while IAE rates were much less impacted by such small additions of O₂.

The effect of frequency and duty cycle of a pulsed negative DC bias voltage was also investigated with a constant 0.25 SCCM O₂ added (Fig. 5). For ion energies above the threshold, the etching rate for 10 kHz pulse frequency was on average higher at 90% duty cycle than at 50% duty cycle, within the expected rise of $<9/5$ increase in the rate expected from the 9/5 increase average flux of energetic ions responsible for IAE, added to a near-constant background of PAE. Decreasing the bias frequency from 10 kHz to 1 Hz at the 50% duty cycle produces a substantial drop in etching rate (roughly twofold). For an interpretation of this result, see Sec. III C.

B. Surface analysis after etching

After etching in the Ar/Cl₂/O₂ plasma, Si samples were transferred to the XPS chamber, under vacuum, for surface analysis. Figure 6 shows XPS low resolution spectra after etching in a 225/25/1 SCCM Ar/Cl₂/O₂ plasma. The spectra consist of only Si, Cl, and O. Spectra were recorded after etching in plasmas containing 0.1–5 SCCM O₂ with the sample either grounded or RF-biased to obtain -65 V self-bias. There was no surface O detected by XPS when a sample was exposed to a baseline Ar/Cl₂ plasma (see Fig. 7, where [O] is zero when the O₂ flow rate was 0 SCCM). Relative surface atom densities, found by integrating the corresponding peak intensities, were used to compute the composition of the SiO_xCl_y film that forms in the presence of oxygen.

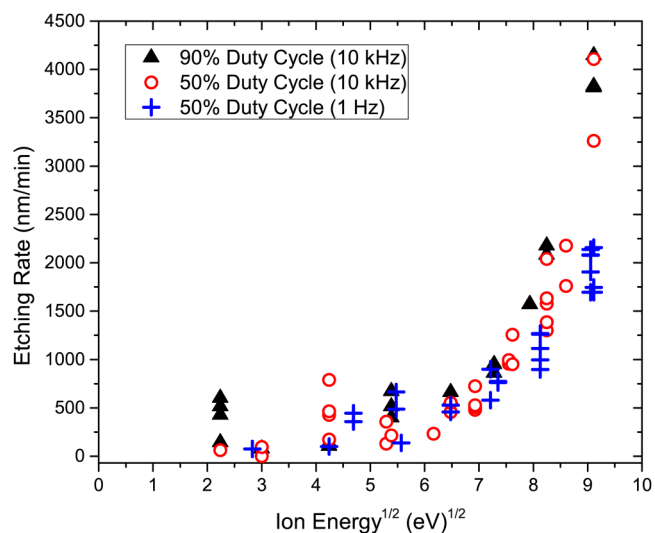


FIG. 5. Etching rate of p-type silicon as a function of the square root of ion energy for different pulsed DC bias duty cycles and frequencies. 0.25 SCCM O₂ was added to Ar/Cl₂ (225/25 SCCM) plasma.

Figure 7 presents film composition as a function of added O₂ with the stage grounded (i.e., no energetic ion bombardment, PAE condition). Only 0.25 SCCM of O₂ was required to grow a relatively thick layer with a stoichiometry of SiO_{1.8}Cl_{0.3}. This layer suppressed PAE. With further additions of O₂, the Cl content in the layer drops further to about 1/10th that of O.

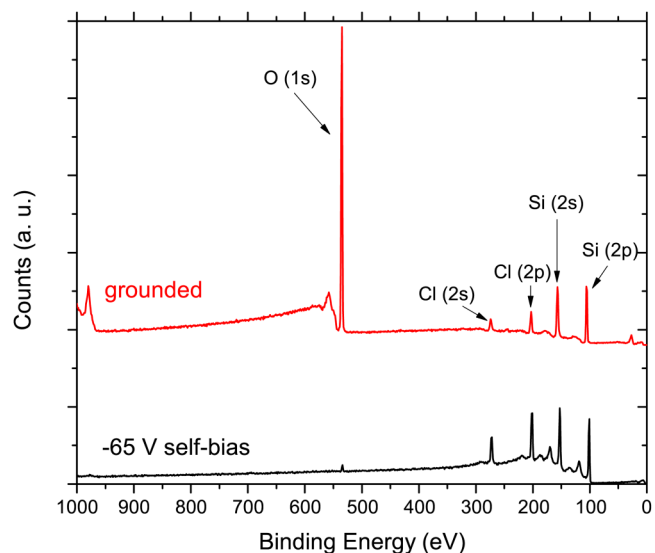


FIG. 6. Low resolution XPS survey spectra (takeoff angle of 30°) of p-type Si after etching in Ar/Cl₂ (225/25 SCCM) plasma with 1 SCCM O₂ added. The sample was etched for 30 s under the PAE condition (grounded stage) or for 10 s under the IAE condition (RF powered stage with -65 V self-bias).

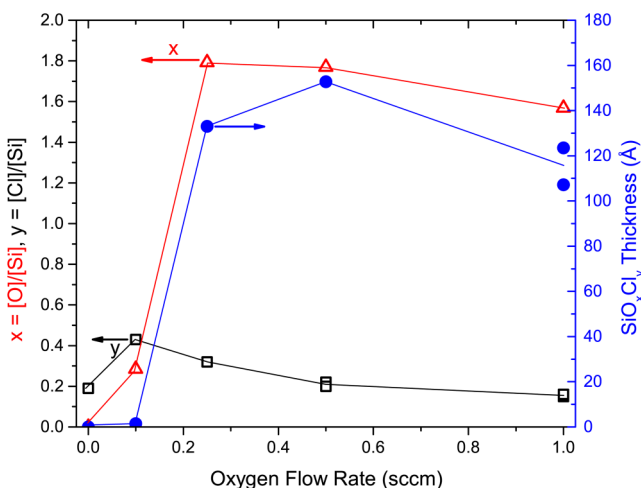


FIG. 7. [O]/[Si] and [Cl]/[Si] atomic concentration ratios (x and y , respectively, open symbols) and the SiO_xCl_y film thickness (solid circles) after etching Si with different flow rates of added oxygen, under PAE conditions (i.e., grounded stage) for 30 s. XPS takeoff angle was 30° for [O]/[Si] and [Cl]/[Si] and 85° for the film thickness determination. A fresh sample was used for each experiment. Data points at 0 SCCM O_2 are taken from our previous work (Ref. 13).

When substantial oxygen was present on the etched surface, high resolution Si(2p) spectra contained the expected peaks of the Si substrate at 99.5 eV and SiO_2 near 104.5 eV, with integrated intensities $I(\text{Si}_{\text{subs}})$ and $I(\text{SiO}_x\text{Cl}_y)$, respectively, where $x \gg y$. Assuming a film of uniform composition SiO_xCl_y , its thickness, d (SiO_xCl_y), can be determined from the intensity ratio of these two peaks by using the following formula:¹⁹

$$d(\text{SiO}_x\text{Cl}_y) = \lambda_{\text{SiO}_2} \sin(\theta) \ln \left\{ 1 + \frac{\lambda_{\text{Si}}}{\lambda_{\text{SiO}_x\text{Cl}_y}} \frac{n_{\text{Si}}}{n_{\text{SiO}_x\text{Cl}_y}} \frac{(1+x+y)I(\text{SiO}_x\text{Cl}_y)}{I(\text{Si}_{\text{subs}})} \right\}, \quad (2)$$

where $\lambda_{\text{SiO}_x\text{Cl}_y}$ and λ_{Si} are electron attenuation lengths for SiO_xCl_y (assumed to be that of SiO_2 , 38 Å)¹⁹ and Si (22 Å),²⁵ respectively, θ is the takeoff angle, $n_{\text{SiO}_x\text{Cl}_y}$ and n_{Si} are the atom densities for the film (assumed to be equal to $6.92 \times 10^{22} \text{ cm}^{-3}$ for SiO_2 and $5.00 \times 10^{22} \text{ cm}^{-3}$ for Si), and x, y refer to the SiO_xCl_y film stoichiometry. The film thickness reported in Figs. 7 and 8 was determined from spectra recorded at takeoff angle $\theta = 85^\circ$. As shown in Fig. 4, PAE stops with addition of 0.5 SCCM oxygen. Figure 7 shows that this corresponds to the presence of a ~130 Å-thick oxide on the surface. Further additions of O_2 to the feed gas produce no increase in film thickness, but a small further decline in the Cl content.

When RF bias power was applied to the stage (-65 V self-bias), oxide formation was suppressed by energetic ion bombardment (not shown). For 1 and 2 SCCM added O_2 , the near-surface composition was $\text{SiO}_{0.03}\text{Cl}_{0.37}$ and $\text{SiO}_{0.05}\text{Cl}_{0.42}$, respectively. 5 SCCM added O_2 resulted in a film with a stoichiometry of $\text{SiO}_{0.64}\text{Cl}_{0.34}$ and a thickness of roughly 20 Å (also not shown), and

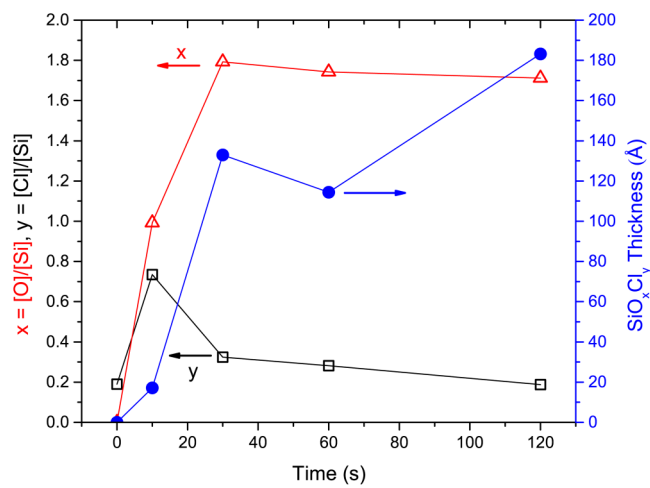


FIG. 8. [O]/[Si] and [Cl]/[Si] atomic concentration ratios (x and y , respectively, open symbols), and SiO_xCl_y film thickness (solid circles) after etching Si for different times, under the PAE condition (i.e., grounded stage) with 0.25 SCCM added O_2 . XPS takeoff angle was 30° for [O]/[Si] and [Cl]/[Si] and 85° for film thickness determination. A fresh sample was used for each experiment. Data points at 0 SCCM O_2 are taken from our previous work (Ref. 13).

the etching rate was reduced by about a factor of ~3 compared to the case of no oxygen addition (see Fig. 3).

For an oxygen addition of 0.25 SCCM, and grounded substrate stage (PAE condition), the SiO_xCl_y layer thickness and the [Cl]/[Si] and [O]/[Si] surface concentration ratios are plotted as a function of etching time in Fig. 8. For short etching times (e.g., 10 s), the oxide layer is relatively thin, and the surface Cl concentration is correspondingly high. For longer etching times (e.g., >30 s) the oxide layer is thick enough to arrest etching. At the same time, the surface becomes severely deficient in Cl. For etching duration of 120 s, the oxide thickness reaches ~180 Å. Without energetic ion bombardment, formation of such thick oxide films stops PAE even for this small amount of 0.25 SCCM of added oxygen ($\text{Cl}_2 : \text{O}_2 = 100:1$ in the feed gas).

C. Implications for steady-state and pulsed-plasma etching of silicon with chlorine

Under steady-state etching conditions, when no RF bias is applied to the substrate, PAE can be suppressed with a very small addition of O_2 (i.e., ≤ 0.5 SCCM added to 25 SCCM of Cl_2 and 225 SCCM Ar feed gas), as indicated by the sub-30 eV ion energy, solid circle points in Fig. 4. On the other hand, with RF bias, PAE can be suppressed while IAE can still occur with the addition of ≤ 5 SCCM O_2 (e.g., 2 SCCM O_2 in 25 SCCM of Cl_2 and 225 SCCM Ar carrier gas at -45 V self-bias voltage on the substrate, as shown in Fig. 2). With energetic ion bombardment, as long as the oxide sputtering rate exceeds the oxidation rate, the depositing layer is sputtered away and PAE can occur, in addition to IAE. Higher ion energies then require more added O_2 to form a thick enough layer to suppress PAE but not IAE. Too much O_2 addition will also stop

IAE. This infers a “window” of the O₂ addition between ~0.5 and 3 SCCM (depending on the ion energy), where IAE occurs with a relatively fast rate but PAE is suppressed. This issue is much more complicated; however, since several processes are entangled. First, the layer that forms with energetic ion bombardment is a suboxide and is thinner than the SiO₂-like layer that grows without energetic ion bombardment. Petit-Etienne *et al.*²⁹ suggested that for very thin oxides (<2.5 nm-thick) in a chlorine plasma, Cl diffuses through the oxide (and/or Cl⁺ ions are implanted through the oxide), leading to a chlorinated layer in the oxide-silicon interface. For high enough levels of chlorination, silicon is etched by releasing SiCl_x species from the surface. For thick oxides, the transport of Cl toward the oxide-silicon interface (and/or the transport of SiCl_x to the surface) is impeded, eventually leading to etch stop. Second, there is evidence that energetic ion bombardment causes damage to the Si substrate that appears to suppress PAE.¹³ If there truly was a window, then one might expect a substantial drop in the etching rate with small O₂ additions (corresponding to the diminishing PAE), a relatively wide region, where the etching rate, dominated by IAE, is nearly constant, and then a rapid drop in the etching rate when IAE cannot clear the depositing oxide layer faster than it grows (for too high oxygen addition). Figure 3 shows hints of this behavior for the single crystal samples (complicated by the initial increase in Cl coverage for ~0.1 SCCM added O₂), but not for polycrystalline Si.

Under pulsed power operation (either source or bias, or a combination of both), if the pulsing frequency is much faster than the time to grow or sputter away the oxide layer, then the dependences of PAE and IAE on O₂ addition would be similar to the continuous wave case. If on the other hand, the pulsing frequency is comparable to or slower than the time to grow or sputter away the oxide layer, then some PAE could occur at the back-end of the power-on fraction of the cycle (while ion bombardment is still on), and at the front-end of the power-off fraction of the cycle (ion bombardment is off), as the oxide film is periodically sputtered away and then regrows.

In Fig. 5, the etching rate with 0.25 SCCM O₂ addition drops by a factor of ~2 in going from 10 kHz to 1 Hz. This can be explained by the etching rate of SiO₂, the plasma oxidation rate of Si, and the dynamics of oxide growth and removal. In our previous study, the SiO₂ film etching rate in a cw Ar/Cl₂ (225/25 SCCM) plasma with continuous RF bias on the stage (resulting in a self-bias of -80 V) was ~6.7 Å/s.¹³ Then scaled to 50% duty cycle, and the somewhat lower negative DC bias used in the present work (-65 V self-bias), the oxide etching rate was at least ~3.3 Å/s (probably larger due to the poor quality of the plasma-oxide layer), meaning ~2 Å of oxide film could be removed during the 0.5 s bias-on duration at 1 Hz. Now, Fig. 8 shows that the initial oxide growth rate is ~20 Å in 10 s or 1 Å in 0.5 s. (The initial oxidation rate is likely faster, so the oxide layer grown in 0.5 s is likely thicker.) Consequently, at 1 Hz, an oxide layer grows during the bias-off part of the period, and it takes roughly half the bias-on portion of the period (~0.25 s) for this oxide to be removed by energetic ion bombardment before etching begins, while at 10 kHz and 50% duty cycle, the much thinner, pseudo-steady-state oxide allows etching during the entire bias pulse period. This would

result in twice the etching rate per minute at 10 kHz, compared to 1 Hz, as observed.

From Fig. 4, it takes ~0.25 SCCM O₂ addition to suppress PAE under steady-state conditions. It is expected that no more than a monolayer or two (<5 Å) would be required to suppress PAE. For the conditions in Fig. 8 (0.25 SCCM oxygen addition), it would, therefore, take <5 s for the oxide layer to thicken enough to suppress PAE. As shown in Fig. 3, an appreciable IAE rate can be obtained at 10 times 0.25 SCCM O₂ addition. If the oxidation rate scales with O₂ addition, then it would be possible to stop PAE in <0.5 s after the cessation of ion bombardment at 2.5 SCCM O₂ addition. Such a very quick cessation of etching is evident in the interferogram in Fig. 2. Again, there are complex interactions between oxidation and ion induced damage. Nonetheless, suppression of PAE relative to IAE could be achieved by small O₂ additions in pulsed-plasma processes, such as atomic layer etching.

IV. SUMMARY AND CONCLUSIONS

The effect of oxygen addition on the in-plasma PAE of *p*-type Si in a Faraday-shielded, Ar/Cl₂ (225 SCCM/25 SCCM), high density, inductively coupled plasma at 60 mTorr was investigated. The etching rate of Si was measured *in situ* by laser interferometry. The etched samples were transferred under vacuum to an XPS chamber for surface analysis, using both survey and high resolution spectra. The thickness and composition of a silicon oxychloride SiCl_xO_y layer, deposited when oxygen was added to the plasma, was determined, using XPS.

The silicon etching rate was measured under both PAE condition (grounded sample stage, low energy ~5 eV ions) and IAE condition (RF or pulsed negative DC powered sample stage, and higher energy ions). Relatively small O₂ additions (e.g., 0.5 SCCM) to the Ar/Cl₂ plasma, stopped PAE with much smaller reductions in the IAE rate. In fact, there is a window of oxygen addition that seems to allow some suppression of PAE, relative to IAE, but the effect is complicated by an apparent suppression of PAE by ion bombardment, reported previously.¹³ With 0.5 SCCM O₂ addition, under PAE conditions (grounded sample), a relatively thick (>120 Å) oxide layer formed on the Si surface, stopping etching. SiO_xCl_y films grown under PAE conditions were much richer in oxygen compared to films grown under IAE conditions.

ACKNOWLEDGMENTS

This work was supported financially by the National Science Foundation (No. PHY-1500518) and the Department of Energy, Office of Fusion Energy Science (No. DE-SC0001939).

REFERENCES

- ¹V. M. Donnelly and A. Kornblit, *J. Vac. Sci. Technol. A* **31**, 050825 (2013).
- ²K. J. Kanarik, T. Lill, E. A. Hudson, S. Sriraman, S. Tan, J. Marks, V. Vahedi, and R. A. Gottscho, *J. Vac. Sci. Technol. A* **33**, 020802 (2015).
- ³B. Wu, A. Kumar, and S. Pamarthi, *J. Appl. Phys.* **108**, 051101 (2010).
- ⁴J. W. Coburn and H. F. Winters, *J. Appl. Phys.* **50**, 3189 (1979).
- ⁵H. Okano, Y. Horike, and M. Sekine, *Jpn. J. Appl. Phys.* **24**, 68 (1985).
- ⁶F. A. Houle, *Phys. Rev. B* **39**, 10120 (1989).
- ⁷W. Sesselmann, E. Hudczek, and F. Bachmann, *J. Vac. Sci. Technol. B* **7**, 1284 (1989).

- ⁸R. Kullmer and D. Bauerle, *Appl. Phys. A* **386**, 377 (1988).
- ⁹S.-B. Wang and A. E. Wendt, *J. Vac. Sci. Technol. A* **19**, 2425 (2001).
- ¹⁰H. Shin, W. Zhu, V. M. Donnelly, and D. J. Economou, *J. Vac. Sci. Technol. A* **30**, 021306 (2012).
- ¹¹W. Zhu, S. Sridhar, L. Liu, E. Hernandez, V. M. Donnelly, and D. J. Economou, *J. Appl. Phys.* **115**, 203303 (2014).
- ¹²S. Sridhar, L. Liu, E. W. Hirsch, V. M. Donnelly, and D. J. Economou, *J. Vac. Sci. Technol. A* **34**, 61303 (2016).
- ¹³E. W. Hirsch, L. Du, D. J. Economou, and V. M. Donnelly, *J. Vac. Sci. Technol. A* **38**, 023009 (2020).
- ¹⁴S. Tian, V. M. Donnelly, and D. J. Economou, *J. Vac. Sci. Technol. B* **33**, 030602 (2015).
- ¹⁵T. Meguro, M. Hamagaki, S. Modaressi, T. Hara, Y. Aoyagi, M. Ishii, and Y. Yamamoto, *Appl. Phys. Lett.* **56**, 1552 (1990).
- ¹⁶S. D. Athavale, *J. Vac. Sci. Technol. B* **14**, 3702 (1996).
- ¹⁷C. J. Mogab, A. C. Adams, and D. L. Flamm, *J. Appl. Phys.* **49**, 3796 (1978).
- ¹⁸S. Taylor, J. F. Zhang, and W. Eccleston, *Semicond. Sci. Technol.* **8**, 1426 (1993).
- ¹⁹V. M. Donnelly, F. P. Klemens, T. W. Sorsch, G. L. Timp, and F. H. Baumann, *Appl. Phys. Lett.* **74**, 1260 (1999).
- ²⁰G. C. H. Zau and H. H. Sawin, *J. Electrochem. Soc.* **139**, 250 (1992).
- ²¹M. Tuda, K. Shintani, and J. Tanimura, *Appl. Phys. Lett.* **79**, 2535 (2001).
- ²²S. Kuroda and H. Iwakuro, *J. Vac. Sci. Technol. B* **16**, 1846 (1998).
- ²³C. C. Cheng, K. V. Guinn, V. M. Donnelly, and I. P. Herman, *J. Vac. Sci. Technol. A* **12**, 2630 (1994).
- ²⁴M. Tuda and K. Ono, *Jpn. J. Appl. Phys.* **36**, 2482 (1997).
- ²⁵N. Layadi, V. M. Donnelly, and J. T. C. Lee, *J. Appl. Phys.* **81**, 6738 (1997).
- ²⁶M. Sternheim, W. Van Gelder, and A. W. Hartman, *J. Electrochem. Soc.* **130**, 655 (1983).
- ²⁷V. M. Donnelly and J. A. McCaulley, *J. Vac. Sci. Technol. A* **8**, 84 (1990).
- ²⁸J. P. Chang, J. C. Arnold, G. C. H. Zau, H.-S. Shin, and H. H. Sawin, *J. Vac. Sci. Technol. A* **15**, 1853 (1997).
- ²⁹C. Petit-Etienne *et al.*, *J. Vac. Sci. Technol. B* **29**, 051202 (2011).